Eye State Detection Using Frequency Features
from 1 or 2-Channel EEG

Francisco Laport, Adriana Dapena*, Paula M. Castro,
Daniel I. Iglesias and Francisco J. Vazquez-Araujo
CITIC Research Centre & University of A Coruña,
Campus de Elviña, s/n A Coruña, 15071, Spain
**adriana.dapena@udc.es*

Brain–computer interfaces (BCIs) establish a direct communication channel between the human brain and external devices. Among various methods, electroencephalography (EEG) stands out as the most popular choice for BCI design due to its non-invasiveness, ease of use, and cost-effectiveness. This paper aims to present and compare the accuracy and robustness of an EEG system employing one or two channels. We present both hardware and algorithms for the detection of open and closed eyes. Firstly, we utilize a low-cost hardware device to capture EEG activity from one or two channels. Next, we apply the discrete Fourier transform to analyze the signals in the frequency domain, extracting features from each channel. For classification, we test various well-known techniques, including Linear Discriminant Analysis (LDA), Support Vector Machine (SVM), Decision Tree (DT), or Logistic Regression (LR). To evaluate the system, we conduct experiments, acquiring signals associated with open and closed eyes, and compare the performance between one and two channels. The results demonstrate that employing a system with two channels and using SVM, DT, or LR classifiers enhances robustness compared to a single-channel setup and allows us to achieve an accuracy percentage greater than 95% for both eye states.

Keywords: Brain–computer interfaces; electroencephalography; eye states; prototype.

1. Introduction

Brain–computer interfaces (BCIs) can be defined as communication systems that monitor the user's brain activity with the aim of translating thoughts into commands.[1–3] Since BCIs allow users to control external devices without the involvement of peripheral nerves and muscles, they are especially useful for people suffering from severe motor disabilities who have lost all motor functions, such as those affected by advanced stages of Amyotrophic Lateral Sclerosis (ALS) or high levels of tetraplegia.[4,5]

The beginning of BCI can be traced back to the 1920s when the German scientist Hans Berger discovered that brain activity generates electrical currents. He demonstrated that the fluctuations of these currents could be recorded by placing electrodes on the scalp of subjects.[6] However, Berger's work primarily focused on utilizing this technique for

---

studying and analyzing cognitive functions, as well as understanding and diagnosing various neuro-pathologies. It was in the 1960s when Joseph Kamiya demonstrated that subjects could exert control over certain characteristics of brain waves after under-going training.[7] Furthermore, Thelma Estrin indicated the significance of electroencephalography (EEG) devices being capable of continuous signal digitization and immediate transmission to computers.[8] In 1973, Vidal introduced the term "Brain–computer interface" and described BCI as the use of brain signals for dialogue between human and computer and as a means of control over external processes such as computers or prosthetic devices.[9] These ideas brought about a revolution in the field of neuroscience and opened up new frontiers and possibilities in various domains, including education, healthcare, and many others.[10]

EEG has emerged as the most popular neuroimaging method for current BCIs due to several advantages it offers, including non-invasiveness, ease of use, and affordability. Traditionally, EEG technology has primarily been employed in medical applications where high measuring accuracy is essential, necessitating the use of devices with multiple channels. However, the high cost and complexity associated with medical-grade EEG devices make them impractical for non-medical applications such as wellness, healthcare, and entertainment.

The rapid advancement of non-medical EEG systems has sparked the development of new applications aimed at assisting individuals in their daily lives. These applications encompass a wide range of areas, including healthcare,[11,12] emotion recognition,[13] or Internet-of-Things (IoT).[14] However, there is limited research concerning the utilization of only one or two channels for BCIs.

In this paper, we present a two-channel system by extending the prototype presented in a previous work.[15] Signals are acquired by replicating the hardware but adding only one additional electrode. The discrete Fourier transform is used to determine relevant features and then evaluate the performance of four classification algorithms: Linear Discriminant Analysis (LDA), Support Vector Machine (SVM), Decision Tree (DT), and Logistic Regression (LR). By employing two channels, our aim is to capture more comprehensive and reliable information from

brain activity, ultimately leading to potential improvements in classification accuracy.

This paper is organized as follows. In Sec. 2, we present a review of previous works in BCI. In Sec. 3, we present a detailed description of our EEG-based system for detecting eye states. This section outlines the architecture and components of our prototype. We explain the data acquisition process, including electrode placement and signal recording techniques. Additionally, we describe the signal processing methods and the classification algorithms used for eye state determination. Section 4 focuses on the study conducted to evaluate the performance of our system. We present the experimental setup and methodology employed in this study. Results and findings from the performance evaluation study are presented and discussed in this section. Finally, in Sec. 5, we offer concluding remarks based on the findings and insights derived from our study.

2. State of the Art

Over the last few decades, the utilization of EEG for BCI has garnered significant interest. In the literature, several reviews on EEG-based BCI systems have been found, encompassing topics such as signal acquisition, preprocessing or signal enhancement, feature extraction, classification methods, and the control interface.[16–18]

BCIs have numerous applications, particularly for individuals with nervous system injuries like ALS, Parkinson's, spinal cord injury, stroke, and consciousness disorders.[11] They show promise in rehabilitation, inducing cortical reorganization through neuronal plasticity for therapeutic benefits. Wearable technology enables in-home monitoring, assessment, and rehabilitation for brain and spinal cord injury patients.[12] However, more studies are needed to demonstrate real improvements, especially for patients with compromised comfort due to a high number of sensors.[19]

EEG-based BCI systems have been also used for emotion recognition.[13] By analyzing the patterns and neural responses associated with different emotional states, EEG signals open up new possibilities for empathetic and responsive technology, paving the way for innovative applications in fields such as healthcare, gaming, marketing, and more.

On the other hand, the integration of low-cost EEG devices with IoT platforms holds great promise in numerous domains, such as smart homes, healthcare, or gaming, among others.[14]

Despite all this progress, the cost of BCI technology remains a limiting factor in its widespread utilization. A recent study[20] aimed to compare the performance of two EEG devices, namely, a low-cost BCI and a high-end EEG, in detecting four emotional conditions. Although the professional-grade EEG device outperformed the low-cost BCI in terms of classification accuracy, both devices demonstrated noteworthy performance in classifying the four emotional conditions.

The successful implementation of BCI systems based on EEG goes beyond technical aspects since designing a comfortable and user-friendly system is crucial. Despite the importance of user comfort, previous works have largely focused on using multiple sensors, overlooking the potential benefits of utilizing one or two channels. Recent research has started to explore the advantages of a reduced number of sensors in EEG-based BCIs for various applications, showcasing the significance of designing user-friendly and cost-effective BCI systems for a wide range of users:

- Shalash *et al.*[21] conducted research to detect fatigue using EEG signals from seven channels. They achieved good accuracy using just a single sensor placed in a position commonly associated with alpha and beta rhythms linked to fatigue and eye movements.
- Educational research involving Neurosky MindWave, which utilizes a single sensor, explored attention levels in autonomous e-learning environments.[22,23]
- Using also Neurosky MindWave, Chen *et al.*[24] identified high and low levels of attention among students, while Patsis *et al.*[25] assessed user attention during Tetris gameplay, examining the relationship between attention and game difficulty.
- Vourvopoulos *et al.*[26] investigated user adaptation in brain-controlled systems, evaluating robot control in real and virtual environments using brainwave signals. These studies exemplify the applications of EEG signals in researching attention levels, cognitive performance, and device control through BCIs.

- Ali *et al.*[27] introduced a novel approach to mental health wellness using Neurosky MindWave. Their study explores the use of brain rhythms to assess and enhance psychological well-being, showing promise for innovative BCI applications.
- Mathe *et al.*[28] employed Neurosky MindWave to estimate the user's depression level as part of a BCI application. The IoT ecosystem associated with this application notified caretakers about the user's mental state.
- In another study related to IoT, Narayana *et al.*[29] utilized Neurosky MindWave to develop a BCI application on an Android phone. This allowed users to lock and unlock a wheelchair and control its movements within an IoT environment.

It is noteworthy that previous studies focusing on the utilization of a limited number of sensors have relied on commercial devices. However, these approaches suffer from a significant drawback due to their inherent limitations. For instance, the Neurosky MindWave device does not allow for the addition of more channels, or changing electrode placements, and operates with proprietary software. This limitation poses a serious challenge for researchers and practitioners seeking to enhance the capabilities and flexibility of their BCI systems.

Taking this into mind, the focus of this paper is to examine the potential benefits of using two channels in BCI systems and whether it can lead to improved system performance in terms of accuracy and robustness compared to the use of only one channel. The specific task under study is the detection of open and closed eyes. To conduct this research, the authors refer to a previous study conducted by Laport *et al.*,[15] which likely explored the same task but for a single channel.

3. Proposed Systems

3.1. *Brain rhythms*

Brain waves are typically described in terms of six frequency bands which correspond to specific mental states.[10] Numerous studies have provided evidence that the alpha rhythm, between 8 Hz and 12 Hz, is prominent in the occipital area of the brain when individuals keep their eyes closed.[30–32] However, this alpha rhythm is diminished when visual stimulation occurs.[33,34]

Beta rhythm is observed in frontal and central regions of the scalp, and it is associated to motor activities. It ranges between 12 Hz and 30 Hz and is symmetrically distributed when there is no motor activity and desynchronized when real movements or motor imagery occur.[1] It is also related to alertness and visual attention over parieto-occipital regions and its attentional-related enhancement is typically accompanied by a decrease of alpha rhythm over occipital areas.[35]

For this reason, following the 10–20 International System (IS)[9] for electrode placements depicted in Fig. 1, it is common practice to position the input channels of the EEG device in the O1 and O2 locations to detect visual activities.

In the proposed system, brain waves are recorded by measuring the potential differences between electrode placements in O1 and O2, with a reference electrode placed in Fp2. The ground electrode is placed in A2.
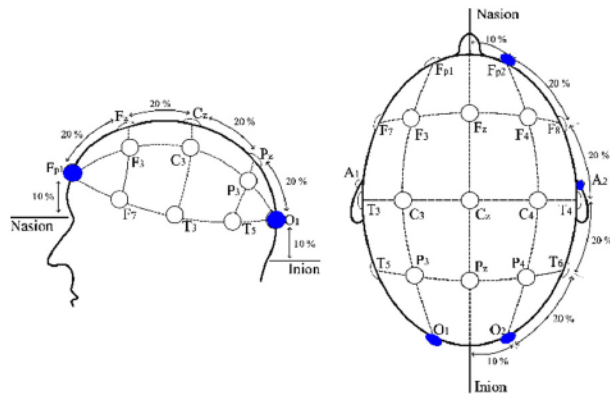

Fig. 1. Electrode placement according to the 10–20 IS.

3.2. Hardware

Figure 2 shows the configuration of the prototype for one or two channels. We can observe that extending to two channels only requires adding one additional electrode and its corresponding amplifier. Thus, the configuration with two channels has a total of four electrodes: two inputs, the reference, and the ground. Each channel uses one input signal, the reference, and the ground.

As explained in our previous work,[15] the signal is amplified by an AD8221 instrumentation amplifier and filtered by a 50 Hz notch filter, a second-order low pass filter, a second-order high pass filter, and a final band pass filter. The gain of this last filter can be adjusted to better utilize the whole range of the analog–digital converter.

The overall filter response is shown in Fig. 3. The filter was designed so that alpha and beta bands are attenuated as little as possible, since they will be employed in the detection of eye states. The notch filter, added to avoid a strong line interference from affecting other frequencies (due to Analog-to-Digital Converter (ADC) saturation) slightly attenuates the upper frequencies of the beta band. However, this does not significantly affect the performance of the system, since we only use the lower portion of the beta band, as we will explain in the following section.

Once the brain signal has been captured, amplified, and filtered, the ESP32 microcontroller is responsible for its digitization. The microcontroller has an ADC with 12-bit resolution. The sampling frequency was configured at 200 Hz. Data captured and processed by the ESP32 is transmitted to an external device (PC or IoT device) using Message Queue
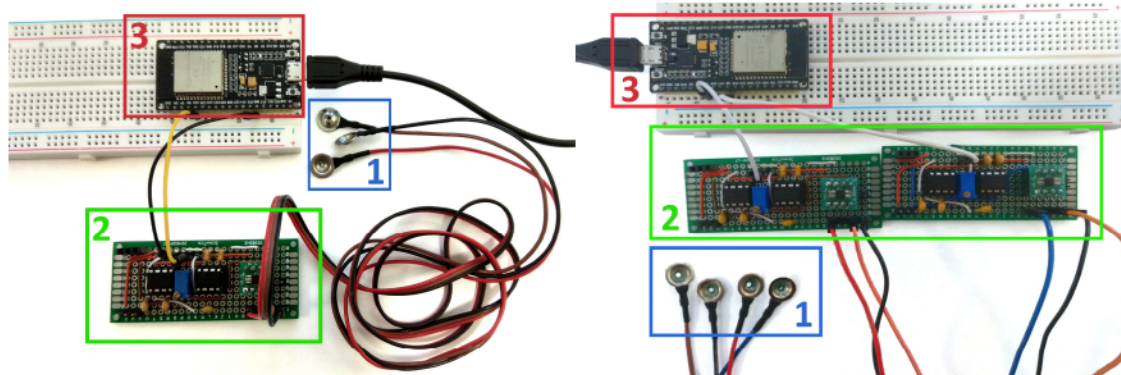

Fig. 2. Prototype with one and two channels: (1) electrodes; (2) amplifiers and filters; and (3) ESP32.
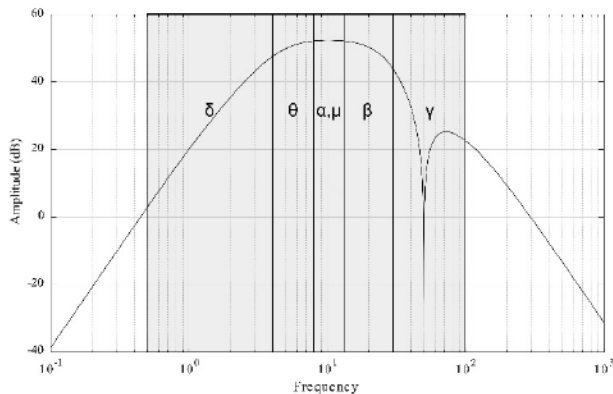
Fig. 3.   Bandpass filter response.

Fig. 4.   Schematic representation of data processing.

Telemetry Transport (MQTT) protocol,[36] a simple and lightweight publish/subscribe messaging protocol designed for constrained devices and low-bandwidth networks. It is easy to implement and can be deployed using open-source solutions such as Eclipse Mosquitto.[37]

There are two different design approaches for the system: (1) the ESP32 transmits the captured samples directly to that control unit, which is responsible for processing and classifying the signal; (2) the algorithms run in the ESP32. In this work, we followed approach (1) because it allowed us to better analyze the captured signals and to study the classification algorithms in more detail.

3.3. *Method for feature extraction*

Signal processing algorithms play a crucial role in extracting meaningful features from the acquired brain signals. The aim is to identify specific patterns in cerebral activity that correspond to different mental states and intentions of the user. However, selecting an appropriate feature set is a complex and challenging task due to the presence of numerous simultaneous brain signal sources and the inherent noise in the environment.

The acquired data are processed as depicted in Fig. 4, where we consider M windows of L samples delayed by P samples.

Considering a window of L samples at time instant m, the Discrete Fourier Transform (DFT) is defined as:

$$X[k,m] = \sum_{n=0}^{L-1} x(m+n)e^{-\frac{j2\pi kn}{L}}, \qquad (1)$$
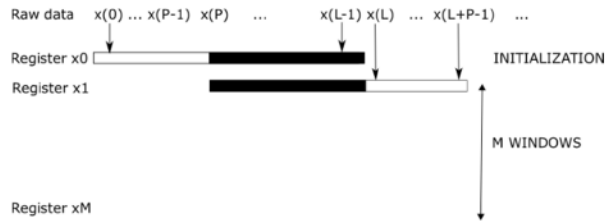
where $k = 0, 1, \ldots, L-1$ represents the frequency bin. Equation (1) may be efficiently implemented using the fast Fourier transform (FFT) algorithm, with a complexity of $O(L\log(L))$ per window.[38] However, we can exploit the relationship between the DFT of consecutive windows to further reduce the complexity by using the sliding DFT algorithm.[39]

For two consecutive windows that are a single sample apart, the DFT can be efficiently computed using the following expression[39]:

$$\begin{aligned} X[k,m+1] &= (X[k,m] - x(m))e^{\frac{j2\pi k}{L}} \\ &\quad + x(m+L)e^{-\frac{j2\pi k(L-1)}{L}} \\ &= (X[k,m] - x(m) + x(m+L))e^{\frac{j2\pi k}{L}}. \quad (2) \end{aligned}$$

This can be executed every time a new sample is received, and it does not involve the use of a sample register. For an interval of P samples, Eq. (2) needs to be computed P times but unlike the FFT, the sliding DFT can be used to calculate only a subset $L_{\alpha\beta}$ of the L frequency bins. This results in a complexity of $O(L_{\alpha\beta}P)$ per window.

As explained before, we are only interested in the frequencies associated with the alpha and beta bands. To reduce the number of operations and ensure synchronization, both bands were selected to have the same number of frequency bins: alpha from 8 Hz to 12 Hz and beta from 13 Hz to 17 Hz. Since the sampling frequency is 200 Hz, $L_{\alpha\beta} = 0.04L$.

Subsequently, we calculate the power of the alpha and beta bands for each channel. Specifically, we obtain $P_{\alpha 1}$ and $P_{\beta 1}$ for channel O1, and $P_{\alpha 2}$ and $P_{\beta 2}$ for channel O2. Finally, we compute the following rates to obtain one feature for each channel.

$$R_1 = \frac{P_{\beta 1}}{P_{\alpha 1}}, \quad R_2 = \frac{P_{\beta 2}}{P_{\alpha 2}}. \qquad (3)$$

3.4. *Methods for feature classification*

The last step of the EEG-based BCI is the feature classification, whose main objective is to detect the user intentions by making use of the previously extracted features (i.e. to identify open eyes and closed eyes). We consider four feature classification algorithms: SVM, LDA, DT, and LR. All these algorithms present a low computational load and are adequate for binary classification.[10,16,40–42] There exist numerous libraries to implement these algorithms in Personal Computer (PC) or microcontrollers.[43,44]

In this section, we provide a concise summary of these algorithms. More detailed explanation can be consulted in the literature.[45]

3.4.1. *SVM*

SVM was first introduced by Vapnik and his team at AT&T Bell Laboratory.[46] SVM seeks a hyperplane or a set of hyperplanes that efficiently separate the features vector into several classes. These hyperplanes must maximize their distance to the closest training samples. The parameters b and $\boldsymbol{w}$ of the hyperplane are obtained by solving the optimization problem. SVM can utilize various types of kernel functions, with our particular focus being on the application of a linear kernel because the problem is linearly separable.

In the classification step, for the feature vector $\boldsymbol{r}(n) = [R_1(n), R_2(n)]^T$, the eye state is determined using a very simple rule:

$$\text{sign}(\boldsymbol{w}\,\boldsymbol{r}(n) + b) > 0 \text{ then ``open eyes''}$$
$$\text{and ``closed eyes'' otherwise.}$$

Appendix A offers a detailed explanation of integrating SVM with the sliding DFT algorithm explained in the preceding section.

3.4.2. *LDA*

LDA is a versatile statistical and machine learning technique applied for dimensionality reduction and supervised classification tasks.[45] Its primary objective is to uncover an optimal linear combination of features or variables that effectively discriminate between two or more distinct classes or groups within a given dataset. To achieve this, LDA begins by computing class averages from the samples, which, in our specific context, corresponds to closed eyes and open eyes states. Additionally, LDA calculates covariance matrices and subsequently derives a projection vector and bias values. During the classification phase, LDA employs a rule similar to SVM to make informed class assignments.

3.4.3. *DT*

DT for binary classification is a machine learning model that employs a tree-like structure to classify data into one of two categories.[45] The DT is obtained through a training process, where it begins with a root node representing the entire dataset and subsequently divides the data recursively based on specific features. The splitting criteria are designed to optimize classification accuracy. Once trained, the DT efficiently predicts the class of new data points.

3.4.4. *LR*

LR is primarily intended for predicting continuous numerical values in regression tasks. Nevertheless, it can be repurposed for binary classification through a thresholding approach.[45] LR starts by structuring the dataset with binary labels. Following this, it applies linear regression to the dataset, and fine-tune the threshold based on the specific problem requirements and the trade-off between precision and recall. This threshold subsequently serves as the basis for classifying data points into their respective classes.

3.4.5. *Other approaches*

In this paper, we have chosen the aforementioned techniques due to their ability to minimize computational overhead while delivering robust performance in solving binary classification problems. In contrast, alternative methods like Artificial Neural Networks (ANNs) and Deep Learning (DL) are better suited for scenarios characterized by a higher number of inputs and multiple classification categories, requiring substantial datasets for effective training.[47–51]

4. Experiments

4.1. *Method*

Seven volunteers agreed to participate in the study. Their mean age was 29.67 years (range 24–56 years).

The participants indicated that they did not have hearing or visual impairments.

Gold cup electrodes were O1 and O2 placed in accordance with the 10–20 IS for electrode placement (see Fig. 1) and attached to the subject scalp using a conductive paste. Electrode-skin impedances were checked to be below $15\,k\Omega$ at all electrodes. The reference and ground electrodes were placed in the Fp2 and A2 positions, respectively, where the absence of hair facilitates their placement, thus optimizing the setup time and EEG signal quality.

The signals were captured using the hardware described in Sec. 3.2, and the signal processing algorithms were executed on a PC using MATLAB, allowing us to repeat the simulations offline with different parameters. However, it is important to emphasize that all these algorithms are also fully implementable on the ESP32 microcontroller.

During the experimental sessions, the signals from the two channels were recorded for a total duration of 10 min per participant. Specifically, the recording process involved 60 s of signal acquisition while the participant had their eyes open, followed by another 60 s of signal acquisition while the participant had their eyes closed. To indicate the transition between the two eye states, a sound alert was played for the participant. Once the electrodes have been placed and the impedance checked to be below $15\,k\Omega$, the recordings started without individual calibration for any of the participants. All the experiments were conducted in a sound attenuated and controlled environment. Participants were seated in a comfortable chair and asked to be relaxed and focused on the task, trying to avoid any distraction or external stimulus. To mimic real-life conditions, the participants were allowed to freely move their gaze during the eye-open tasks, without the requirement of maintaining fixation on a specific point. To reduce possible artifacts, participants were asked not to move or speak during the experiments. After each recording session data for each subject were visually inspected and the recording was repeated if any of them was corrupted by high level of noise or artifacts.

4.2. *Recorded signals*

Figures 5(a) and 5(b), as well as Figs. 6(a) and 6(b), display 10 s of EEG activity, representing open eyes and closed eyes for channel O1 and channel O2,

respectively. The amplitude of the recorded signals by the electrodes is in the microvolt range, varying from a few microvolts to approximately 300 microvolts. Consequently, the acquired EEG signal is highly sensitive to both internal and external noises, including electromagnetic interference generated by nearby devices or various biological signals originating from sources other than the brain (e.g. eyes and jaw).

On the other hand, Figs. 5(c) and 5(d), as well as Figs. 6(c) and 6(d), illustrate these signals in the frequency domain. The alpha band (8–12 Hz) exhibits more pronounced activity during closed eyes, displaying values significantly higher than those observed during open eyes. This observation is also evident in the time domain, where the signals during closed eyes display bursts of alpha activity. Additionally, it can be observed that the beta rhythm (12–30 Hz) does not exhibit significant differences between the two eye states.

As an example of the features obtained with this procedure, Fig. 7 shows the values of R_1 and R_2 for 10 windows of 10 s and a delay of 2 s and 4 s for both eye states. It is evident that the values obtained for closed eyes are significantly lower compared to those for open eyes. This disparity can be attributed to the higher presence of the alpha rhythm during the closed eyes state. The selection of the window size and the temporal gap between windows is a crucial aspect to consider during the design process, as it directly impacts the delay associated with the transmission of control commands and the computational cost of the entire system.

As an illustrative example, Fig. 8 demonstrates the application of the SVM algorithm in estimating the subject's eye state. The plot highlights the support vectors and the classifier's decision boundary. It is evident from the plot that the problem demonstrates linear separability: points situated below the decision boundary predominantly correspond to the closed eye state, while points positioned above the boundary indicate the open eye state. Consequently, a linear kernel has been employed in SVM for this specific scenario.

4.3. *Comparison study*

To compare the performance of a one-channel system and a two-channel system, we conducted an

Fig. 5.   EEG recorded signals from channel O1 for both eye states in the time and frequency domain: (a) open eyes in the time domain; (b) closed eyes in the time domain; (c) open eyes in the frequency domain; (d) closed eyes in the frequency domain.
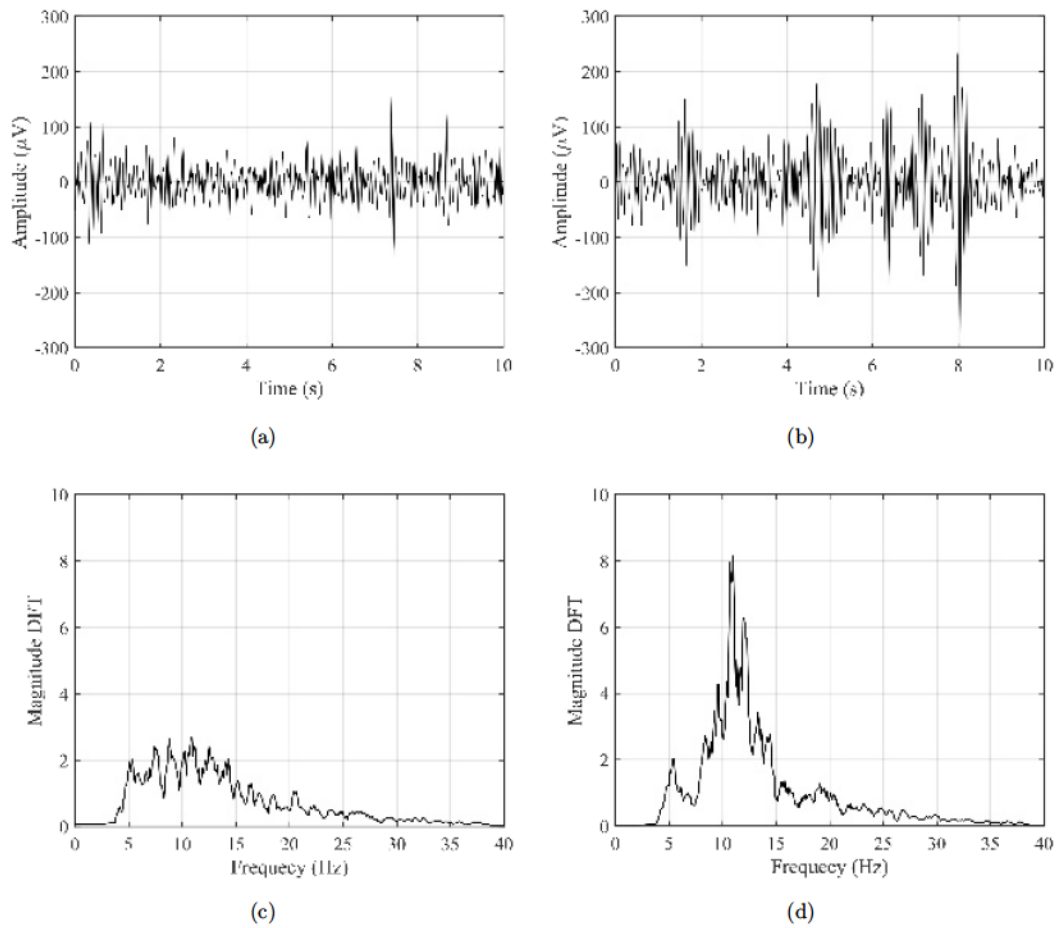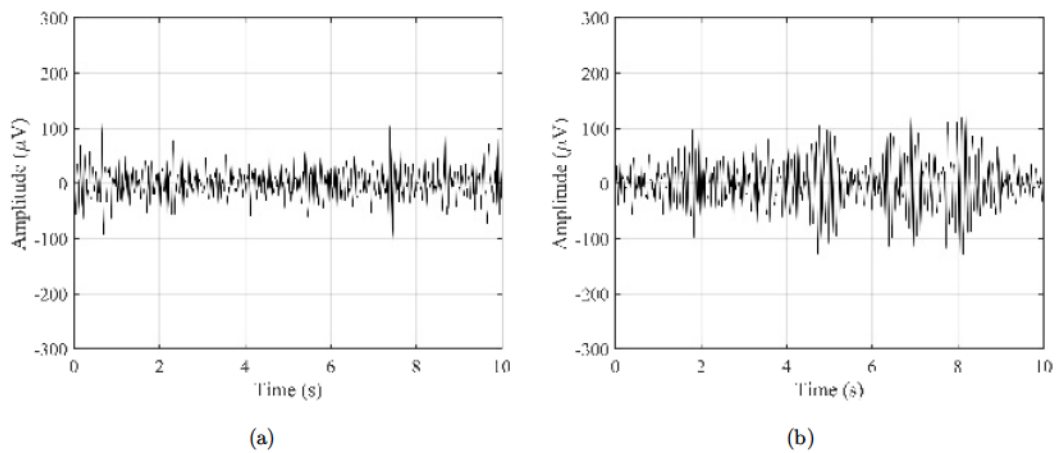

Fig. 6.   EEG recorded signals from channel O2 for both eye states in the time and frequency domain: (a) open eyes in the time domain; (b) closed eyes in the time domain; (c) open eyes in the frequency domain; (d) closed eyes in the frequency domain.

(c)   (d)

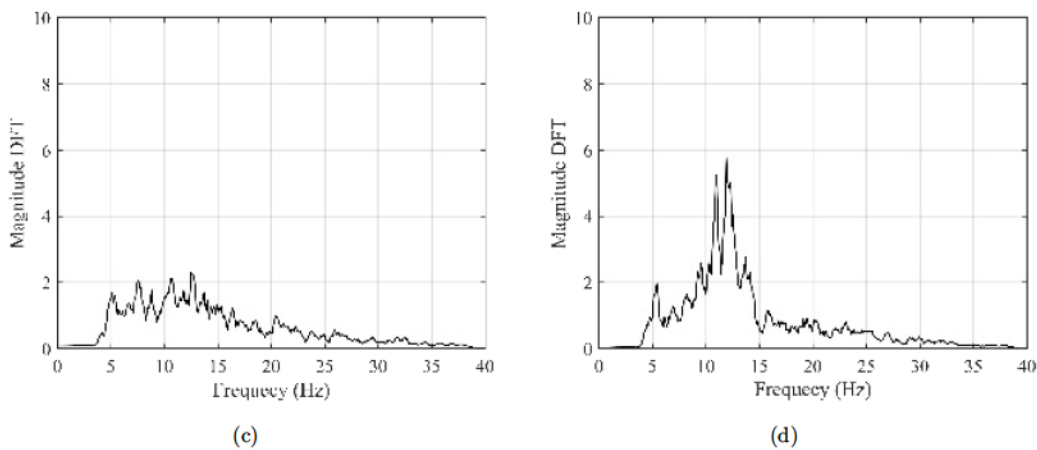Fig. 6.   (*Continued*)

(a)   (b)

(c)   (d)

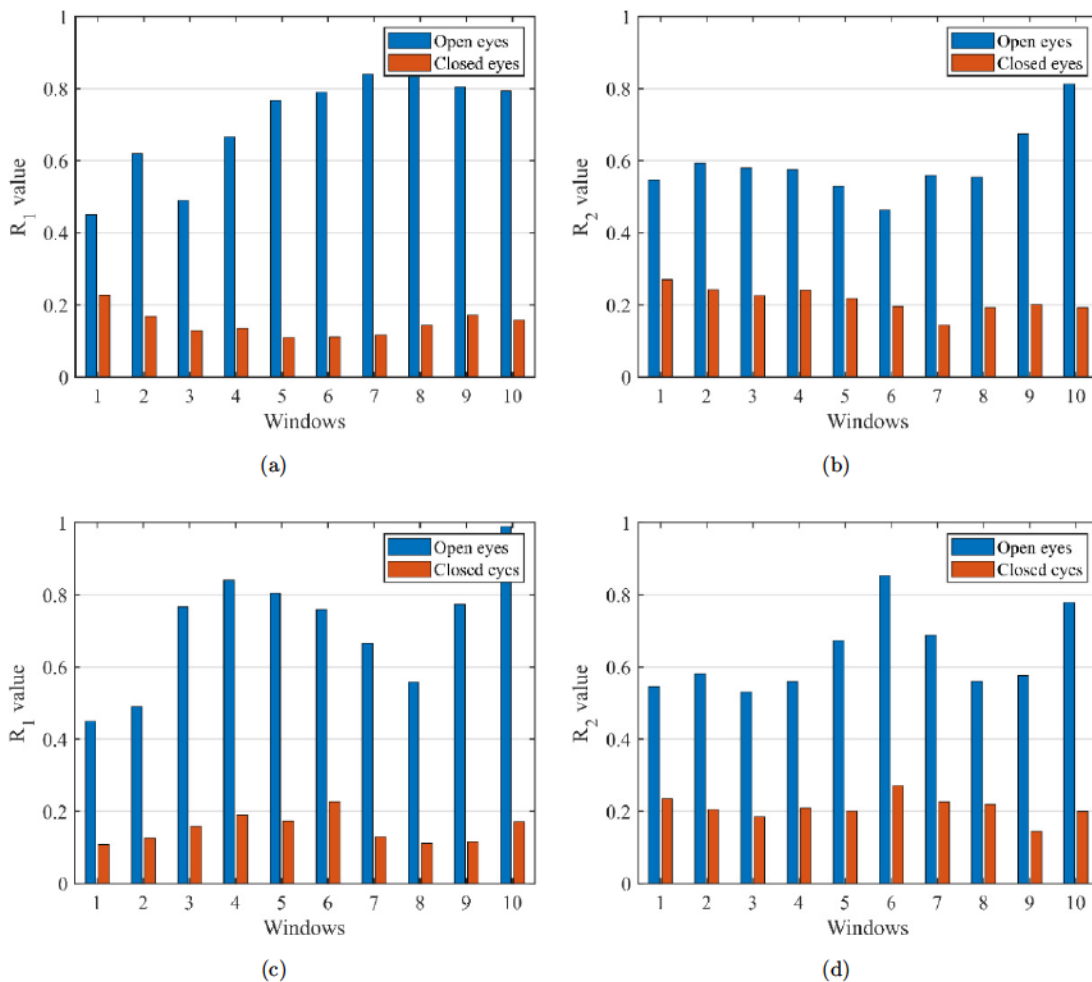Fig. 7.   Ratios R1 and R2 obtained for 10 windows of 10 seconds and two delays: (a) R1 for a delay of 2 s; (b) R2 for a delay of 2 s; (c) R1 for a delay of 4 s; (d) R2 for a delay of 4 s.
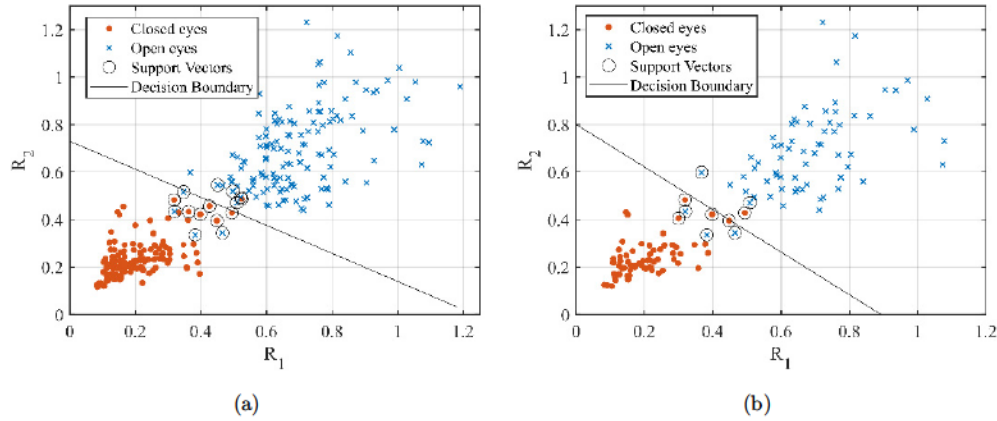
Fig. 8. Extracted features for both eye states and the support vectors and decision boundary employed by the SVM algorithm to perform the classification: (a) delay of 2 s; (b) delay of 4 s.

evaluation to assess their effectiveness in capturing and analyzing EEG signals. In this evaluation, 4 min of the recorded signals are employed for the training step, where two of them correspond to open eyes and two to closed eyes. The remaining 6 min of the recordings, composed by 3 min of each eye state, are employed for the test step.

To mitigate classification bias, we repeated each experiment 10 times using a cross-validation process, i.e. a different combination of training and test recordings is implemented in each of them.

Additionally, for the training step, an inner five-fold cross-validation is performed for tuning the hyperparameters of the classifiers, which is carried out by the Bayesian optimization algorithm.[52]

We considered a window length of 10 s and conducted experiments to determine the optimal delay using delays of 1, 2, 4, and 6 s. It is important to note that the window delay directly influences the computational cost of implementing the sliding DFT in Eq. (2). Since the prototype operates at a sample frequency of 200 Hz, Eq. (2) is updated with $P = 200$ samples (1 s), $P = 400$ samples (2 s), $P = 800$ samples (4 s), or $P = 1200$ samples (6 s). In all cases, $L = 2000$ and $L_{\alpha\beta} = 0.04L = 80$.

Tables 1 and 2 display the mean accuracy for O1 and O2, respectively. It can be observed that the performance is similar for all delays. SVM, LR, and DT classifiers demonstrate the best performance, achieving high average accuracy for both eye states. However, LDA shows low accuracy for open eyes. The shortest delay of 1 s yields good results and ensures the fastest response of the system. Therefore, we will use this value for the remaining experiments.

Table 1. Comparison of classification mean accuracy (in %) for open and closed eyes using O1 and different delays (s).

Delay (s)	SVM	LDA	LR	DT
	Open eyes			
1	94.03	86.40	93.46	94.11
2	93.84	86.40	93.37	93.82
4	92.89	86.39	92.96	93.44
6	92.55	85.67	93.01	93.57
	Closed eyes			
1	93.88	96.79	94.19	93.39
2	93.67	96.78	93.96	93.24
4	93.51	96.87	93.61	92.99
6	93.93	96.58	94.54	93.47

Table 2. Comparison of classification mean accuracy (in %) for open and closed eyes using O2 and different delays (s).

Delay (s)	SVM	LDA	LR	DT
	Open eyes			
1	96.00	88.18	95.29	96.50
2	95.85	87.97	95.11	96.30
4	95.17	87.89	93.91	95.00
6	95.10	88.32	94.74	96.33
	Closed eyes			
1	94.52	97.65	95.09	94.35
2	94.54	97.86	95.15	94.20
4	94.80	97.69	95.54	94.29
6	94.64	97.19	95.26	93.27

Table 3. Comparison of classification accuracy (in %) for open and closed eyes using O1. Bold values indicate the best accuracy per subject.

Subject	SVM	LDA	LR	DT
		Open eyes		
1	**99.87**	97.93	99.51	**99.87**
2	**88.00**	85.03	87.57	85.09
3	**99.57**	93.45	98.24	**99.57**
4	92.24	82.00	91.15	**93.87**
5	**97.63**	96.96	97.27	96.18
6	85.21	67.69	84.06	**88.06**
7	95.63	81.69	**96.42**	96.12
Mean	94.03	86.40	93.46	**94.11**
		Closed eyes		
1	100	100	100	100
2	86.00	**89.74**	87.39	86.48
3	100	100	100	100
4	90.42	**95.39**	91.69	91.15
5	94.78	**97.21**	94.54	94.78
6	87.45	**95.27**	87.75	83.33
7	98.48	**100**	97.93	97.93
Mean	93.88	**96.79**	94.19	93.39

Tables 3 and 4 present the accuracy obtained by each classifier when using a single sensor positioned at O1 and O2, respectively. For the open eyes state, the LDA classifier yields a comparatively lower

Table 4. Comparison of classification accuracy (in %) for open and closed eyes using O2. Bold values indicate the best accuracy per subject.

Subject	SVM	LDA	LR	DT
		Open eyes		
1	**100**	97.39	99.75	**100**
2	94.48	88.72	91.57	**97.21**
3	**100**	95.75	99.81	**100**
4	97.87	86.84	98.36	**98.54**
5	**97.93**	93.39	97.69	97.27
6	89.75	72.00	88.36	**91.39**
7	**91.93**	83,15	91.45	91.09
Mean	96.00	88.18	95.29	**96.50**
		Closed eyes		
1	100	100	100	100
2	88.84	**90.84**	89.75	85.81
3	100	100	100	100
4	98.00	**99.93**	98.30	98.00
5	92.60	**98.12**	94.18	95.69
6	91.45	**96.96**	92.42	90.18
7	90.72	**97.69**	90.96	90.72
Mean	94.52	**97.65**	95.09	94.35

accuracy in comparison with the other classifiers (mean accuracy less than 90%). On the other hand, for the closed eyes state, all classifiers achieve a mean accuracy greater than 90%, indicating good results.

According to Table 4, the results obtained when using a single sensor positioned at O2 show some improvements compared to Table 3, particularly for some subjects. This indicates that SVM, LR, and DT classifiers are consistently effective in classifying EEG signals captured by the sensor at position O2. However, the LDA classifier exhibits a significant difference in mean accuracy between the two eye states. This suggests that the LDA classifier may be more sensitive to the specific characteristics of the signals captured at position O2, leading to variations in its performance.

These results highlight the importance of considering the specific sensor position when evaluating the performance of classifiers. In particular, the results indicate that different sensor positions (in this case, O1 and O2) can yield variations in accuracy and performance for different classifiers.

Table 5 shows the results obtained using two sensors placed on O1 and O2. Comparing with Tables 3 and 4, we see that the performance is similar to when only O2 is used. This suggests that the performance achieved using a two-channel system is

Table 5. Comparison of classification accuracy (in %) for open eyes using two channels. Bold values indicate the best accuracy per subject.

| Subject	SVM	LDA	LR	DT
		Open eyes		
1	99.81	97.69	99.58	**99.88**
2	**91.39**	88.30	90.30	**91.39**
3	**100**	96.84	99.76	99.58
4	97.75	89.45	97.64	**99.09**
5	**97.63**	97.33	97.21	96.55
6	**88.84**	71.09	88.36	88.73
7	95.21	82.96	95.76	**96.12**
Mean	95.81	89.10	95.52	**95.90**
		Closed eyes		
1	100	100	100	100
2	87.51	**90.18**	88.06	84.12
3	100	100	100	100
4	96.90	**99.15**	96.97	91.88
5	95.81	**97.51**	95.52	94.36
6	89.75	**96.48**	90.79	86.61
7	97.03	**100**	97.52	97.94
Mean	95.29	**97.62**	95.55	93.56
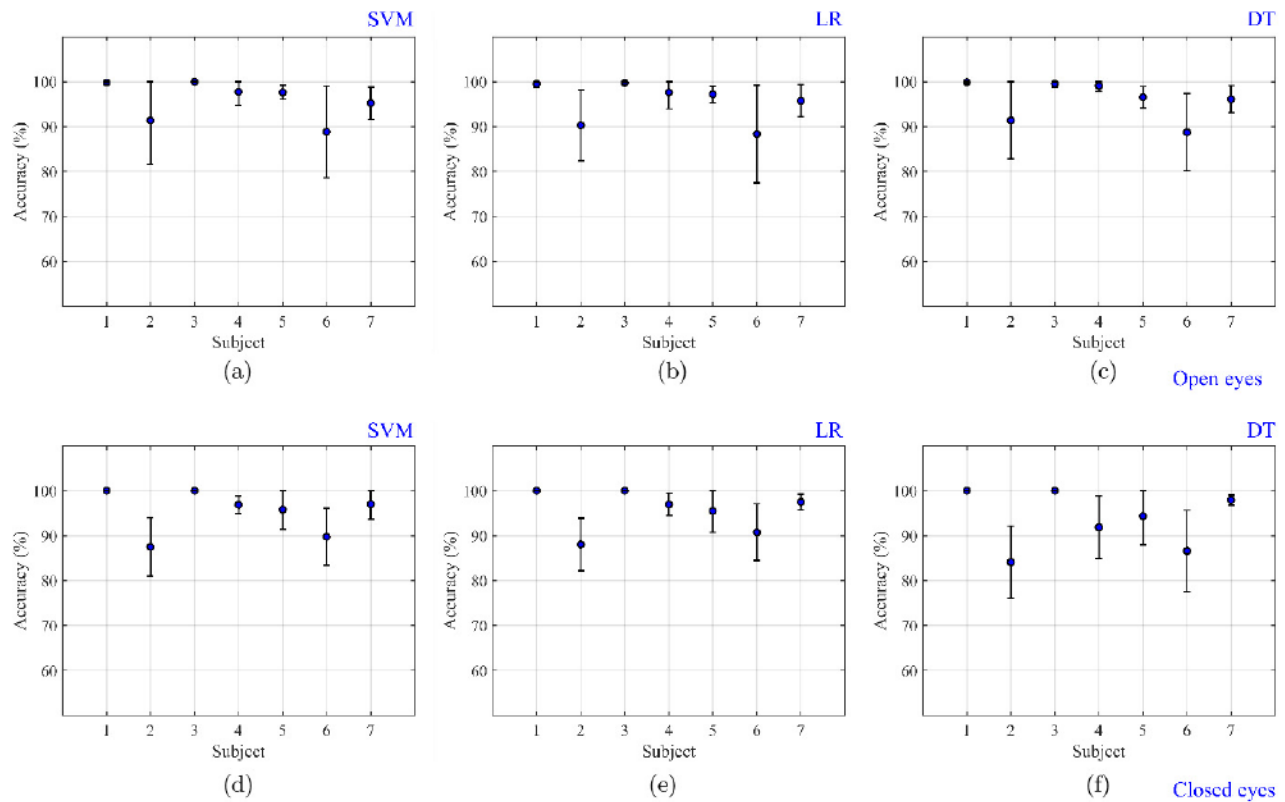
Fig. 9. Mean classification accuracies and standard deviation for each subject and SVM, LR and DT classifiers.

comparable to the performance obtained with the best single sensor position.

It is important to note that the optimal sensor position may vary for different subjects, and it cannot be determined *a priori*. For example, for open eyes and SVM, Subject 2 achieved an accuracy of 88% with position O1 and 94.48% with position O2, and Subject 7 achieved an accuracy of 95.63% with position O1 and 91.93% with position O2. However, it is worth noting that using both sensors (O1 and O2) consistently yields good accuracy. In the case of Subject 2, the utilization of both channels resulted in an accuracy of 91.39%, while for Subject 7, it resulted in an accuracy of 95.21%. These results suggest that combining the information from multiple channels can enhance the overall accuracy of the classification system, even when the optimal single sensor position is uncertain.

Finally, Fig. 9 shows the mean accuracy and standard deviation achieved by SVM, LR, and DT for each user and eye state. The three classifiers offer robust results, as the subjects achieve similar accuracies for both eye states. However, for Subject 2,

accuracy falls below 90% with the three classifiers in the case of closed eyes. For Subject 6, accuracy is also below 90% for the three classifiers with open eyes and for DT with closed eyes. Additionally, the deviation observed for DT when classifying closed eyes is slightly higher compared to the other classifiers.

Based on the analysis of these results, it can be concluded that SVM, LR, and DT exhibit similar results when utilizing two channels (O1 and O2), which makes this the most favorable solution. This indicates that these classifiers effectively capture and utilize the information from both sensor channels to make accurate classifications.

5. Conclusions

In this paper, we present a prototype of an EEG device designed to acquire signals using a reduced number of channels. The hardware consists of cost-effective components, including a dual-core microcontroller that enables us to perform all necessary operations for feature extraction and classification. Our study focuses on determining the user's eye states, specifically

distinguishing between open and closed eyes, by proposing and comparing various algorithms.

Through a comparative analysis of utilizing one versus two channels, our findings indicate that a configuration with two channels provides greater robustness. This observation highlights the advantages of integrating additional sensor data for classification purposes.

We have obtained noteworthy results using the configuration employing two channels in conjunction with SVM, LR, or DT, as the accuracy exceeds 95% for both eye states. However, it is worth noting that when utilizing LDA with two channels, there is a distinct variation in accuracy between the classifications of closed and open eyes.

Considering these results, we can appreciate that the proposed system holds significant potential for applications in non-critical domains. For instance, the prototype can be utilized for detecting fatigue, healthcare, games, or educational purposes. In such domains, the system response time does not need to be shorter than 1 s, and the user's eye state should remain stable without presenting sudden changes in short periods of time.

It is also important to note that, as the main objective of this study was to prove the performance of the proposed BCI system for eye state detection, the analyzed experiments were conducted in a controlled scenario. Therefore, future work will include the study of the proposed BCI system under real-life conditions with a higher noise level and a more realistic eye behavior from the subjects. Additionally, these experiments must include a larger number of participants, especially subjects with mobility disorders. Moreover, since our study is based on alpha activity, which is also related to cognitive and memory tasks,[53,54] future experiments must analyze these scenarios as they may be a source of false positive detections and affect the performance of the system.

Acknowledgments

ORCID

Francisco Laport https://orcid.org/0000-0002-6543-8236

Adriana Dapena https://orcid.org/0000-0001-7362-6854

Paula M. Castro https://orcid.org/0000-0002-0521-3465

Daniel I. Iglesias https://orcid.org/0000-0001-5830-681X

Francisco J. Vazquez-Araujo https://orcid.org/0000-0002-9964-5727

Appendix A. Algorithm with Sliding DFT and SVM

This appendix provides a detailed procedure for conducting feature extraction and classification. We consider the schematic representation of data processing in Fig. 4.

The initial step involves utilizing the register x_0 to load L samples, which is needed for the computation of initial frequency features. To achieve this, the FFT is applied and the results corresponding to alpha and beta bands are extracted:

> Load L samples in x_0
> Compute $X_0 = \text{FFT}(x_0)$,
> Obtain X_α, X_β from X_0.

Subsequently, every time a new sample is obtained, the algorithm updates X_α and X_β. Note that only the frequencies bins corresponding to alpha and beta bands need to be computed:

> For $l = 1$ to P:
>   Load 1 sample in x_m,
>   Set $x_0(1) \ldots x_0(L-1) x_m$,
>   Compute $A_\alpha = X_\alpha - x_0(1) + x_0(L)$,
>   Compute $A_\beta = X_\beta - x_0(1) + x_0(L)$,
>   For $k = 0$ to $L_{\alpha\beta} - 1$:
>   Compute $X_\alpha(k) = A_\alpha e^{\frac{j2\pi(k+\alpha_0)}{L}}$.
>   Compute $X_\beta(k) = A_\beta e^{\frac{j2\pi(k+\beta_0)}{L}}$.

In our case, $f_s = 200$, $L = 2000$, $L_{\alpha\beta} = 80$, $\alpha_0 = 8L/f_s$ and $\beta_0 = 13L/f_s$.

Upon processing P samples, the power of each band is then computed:

For $k = 0$ to $L_{\alpha\beta} - 1$:
   Compute $P_\alpha = P_\alpha + |X_\alpha(k)|^2$,
   Compute $P_\beta = P_\beta + |X_\beta(k)|^2$.

This algorithm is used to calculate the power of both channels. Specifically, it yields the values $P_{\alpha 1}$, $P_{\beta 1}$, $P_{\alpha 2}$ and $P_{\beta 2}$, which are then employed to obtain the corresponding channel power ratios:

Compute $R_1 = P_{\beta 1}/P_{\alpha 1}$,
Compute $R_2 = P_{\beta 2}/P_{\alpha 2}$.

Finally, the classification process is executed. In the case of the SVM classifier, for example, the vector w and bias b derived during the training phase are employed:

Set $\boldsymbol{r} = \text{transpose}\,([R_1, R_2])$,
Compute $s = \text{sign}\,(\boldsymbol{wr} + b)$,
If $s > 0$ then "open eyes"; else "closed eyes".

References

1. G. Pfurtscheller and C. Neuper, Motor imagery and direct brain–computer communication, *Proc. IEEE* **89**(7) (2001) 123–1134, doi: 10.1109/5.939829.

2. A. Ortiz-Rosario and H. Adeli, Brain–computer interface technologies: From signal to action, *Rev. Neurosci.* **24**(5) (2013) 537–552.

3. R. A. Ramadan and A. V. Vasilakos, Brain–computer interface: Control signals review, *Neurocomputing* **223** (2017) 26–44.

4. A. Kübler, N. Neumann, J. Kaiser, B. Kotchoubey, T. Hinterberger and N. P. Birbaumer, Brain–computer communication: Self-regulation of slow cortical potentials for verbal communication, *Arch. Phys. Med. Rehabil.* **82**(11) (2001) 1533–1539.

5. I. H. Iversen, N. Ghanayim, A. Kübler, N. Neumann, N. Birbaumer and J. Kaiser, A brain–computer interface tool to assess cognitive functions in completely paralyzed patients with amyotrophic lateral sclerosis, *Clin. Neurophysiol.* **119**(10) (2008) 2214–2223.

6. H. Berger, Über das elektronkephalogramm des menschen, *Arch. Psychiatr. Nervenkr.* **87**(1) (1929) 527–570 (in German).

7. J. Kamiya, Conscious control of brain waves, *Psychol. Today* **1** (1968) 56–60.

8. T. Estrin, On-line electroencephalographic digital computing system, *Electroencephalogr. Clin. Neurophysiol.* **19**(5) (1965) 524–526.

9. J. J. Vidal, Toward direct brain–computer communication, *Annu. Rev. Biophys. Bioeng.* **2**(1) (1973) 157–180.

10. C. S. Nam, A. Nijholt and F. Lotte (eds.), *Brain–Computer Interfaces Handbook: Technological and Theoretical Advances* (CRC Press, Boca Raton, 2018).

11. A. Burns, H. Adeli and J. A. Buford, Brain–Computer Interface after nervous system injury, *Neuroscientist* **20**(6) (2020) 639–651.

12. A. Burns and H. Adeli, Wearable technology for patients with brain and spinal cord injuries, *Rev. Neurosci.* **28**(8) (2017) 913–920.

13. C. Zhang, Q. Liu, X. Liu and J. Wu, Emotion recognition using EEG signals: A comprehensive review, *IEEE Trans. Affect. Comput.* **8**(4) (2017) 571–586, doi: 10.1109/TAFFC.2016.2535402.

14. J. Smith, A. Johnson and C. Lee, Brain–computer interface for Internet of Things: A comprehensive review, *Int. J. Hum.-Comput. Interact.* **36**(3) (2022) 267–285, doi: 10.1080/10447318.2021.1974525.

15. F. Laport, A. Dapena, P. M. Castro, F. J. Vazquez-Araujo and D. Iglesia, A prototype of EEG system for IoT, *Int. J. Neural Syst.* **30**(07) (2020) 2050018.

16. F. Lotte, M. Congedo, A. Lecuyer, F. Lamarche and B. Arnaldi, A review of classification algorithms for EEG-based brain–computer interfaces, *J. Neural Eng.* **4**(2) (2007) R1–R13, doi: 10.1088/1741-2560/4/2/R01.

17. L. F. Nicolas-Alonso and J. Gomez-Gil, Brain–computer interfaces: A review, *Sensors* **12**(2) (2012) 1211–1279.

18. Y. Zhang, G. Zhou and J. Jin, Recent advances in EEG-based brain–computer interface systems: A systematic review, *Front. Hum. Neurosci.* **15** (2021) 672047, doi: 10.3389/fnhum.2021.672047.

19. D. Salisbury, T. Parsons, K. Monden, Z. Trost and S. Driver, Brain–computer interface for individuals after spinal cord injury, *Rehabil. Psychol.* **61** (2016) 435–441, doi: 10.1037/rep0000099.

20. J. M. Latorre, Fernández-Caballero emotion A, classification from EEG with a low-cost BCI versus a high-end equipment, *Int. J. Neural Syst.* **32**(10) (2022) 2250041.

21. W. M. Shalash, Driver fatigue detection with single EEG channel using transfer learning, in *IEEE Int. Conf. Imaging Systems and Techniques (IST)*, 9–10 December 2019, Abu Dhabi, United Arab Emirates, pp. 1–6, doi: 10.1109/IST48021. 2019.9010483.

22. R. Shadiev, T. T. Wu and Y. M. Huang, Enhancing learning performance, attention, and meditation using a speech-to-text recognition application: Evidence from multiple data sources, *Interact. Learn. Environ.* **25**(2) (2017) 249–261.

23. J. Xu and B. Zhong, Review on portable EEG technology in educational research, *Comput. Humn. Behav.* **81** (2018) 340–349.

24. C. M. Chen, J. Y. Wang and C. M. Yu, Assessing the attention levels of students by using a novel attention aware system based on brainwave signals, *Br. J. Educ. Technol.* **48**(2) (2017) 348–369.

25. G. Patsis, H. Sahli, W. Verhelst and O. De Troyer, Evaluation of attention levels in a tetris game using a brain–computer interface, in *User Modeling, Adaptation, and Personalization*, eds. S. Carberry, S. Weibelzahl, A. Micarelli and G. Semeraro, UMAP 2013, Lecture Notes in Computer Science, Vol. 7899 (Springer, Berlin, Heidelberg), doi: 10.1007/978-3-642-38844-6_11.

26. A. Vourvopoulos and F. Liarokapis, Evaluation of commercial brain–computer interfaces in real and virtual world environment: A pilot study, *Comput. Electr. Eng.* **40**(2) (2014) 714–729.

27. A. Ali, R. Afridi, T. Soomro, A single-channel wireless EEG headset enabled neural activities analysis for mental healthcare applications, *Wirel. Pers. Commun.* **125**(2) (2022) 3699–3713.

28. E. Mathe and E. Spyrou, Connecting a consumer brain–computer interface to an internet-of-things ecosystem, in *Proc. 9th ACM Int. Conf. Pervasive Technologies Related to Assistive Environments* (Association for Computing Machinery, 2016), Article No. 90, pp. 1–2, doi: 10.1145/2910674. 2935844.19.

29. S. Narayana, R. V. Prasad and K. Warmerdam, Mind your thoughts: BCI using single EEG electrode, *IET Cyber-Phys. Syst. Theory Appl.* **4**(2) (2018) 164–172.

30. E. D. Adrian and B. H. C. Matthews, The berger rhythm: Potential changes from the occipital lobes in man, *Brain* **57**(4) (1934) 355–385.

31. R. J. Barry, A. R. Clarke, S. J. Johnstone, C. A. Magee and J. A. Rushby, EEG differences between eyes-closed and eyes-open resting conditions, *Clin. Neurophysiol.* **118**(12) (2007) 2765–2773.

32. R. J. Barry and F. M. De Blasio, EEG differences between eyes-closed and eyes-open resting remain in healthy ageing, *Biol. Psychol.* **129** (2017) 293–304.

33. J. A. Pineda, The functional significance of mu rhythms: translating "seeing" and "hearing" into "doing", *Brain Res. Rev.* **50**(1) (2005) 57–68.

34. A. Gale, N. Dunkin and M. Coles, Variation in visual input and the occipital EEG, *Psychon. Sci.* **14**(6) (1969) 262–263.

35. J. Kamiński, A. Brzezicka, M. Gola and A. Wróbel, Beta band oscillations engagement in human alertness process, *Int. J. Psychophysiol.* **85**(1) (2012) 125–128.

36. J. M. Robinson, J. G. Frey, A. J. Stanford-Clark, A. D. Reynolds and B. V. Bedi, Sensor networks and grid middleware for laboratory monitoring, in *1st Int. Conf. e-Science and Grid Computing (e-Science'05)*,

5–8 July 2005, Melbourne, VIC, Australia, pp. 8–569, doi: 10.1109/E-SCIENCE.2005.73.

37. Eclipse Mosquitto, https://mosquitto.org/.

38. K. R. Rao, S. Do Nyeon and H. Jae Jeong, *Fast Fourier Transform: Algorithms and Applications* (Springer, Dordrecht, 2010).

39. E. Jacobsen and R. Lyons, The sliding DFT, *IEEE Signal Process. Mag.* **20**(2) (2003) 74–80, doi:10. 1109/MSP.2003.1184347SLIDING 2.

40. V. Bahel, S. Pillai and M. Malhotra, A comparative study on various binary classification algorithms and their improved variant for optimal performance, in *IEEE Region 10 Symp. (TENSYMP)*, 5–7 June 2020, Dhaka, Bangladesh, pp. 495–498, doi: 10.1109/TENSYMP50017.2020.9230877.

41. F. Lotte, A tutorial on EEG signal-processing techniques for mental-state recognition in brain–computer interfaces, in *Guide to Brain–Computer Music Interfacing* (Springer, London, 2020), pp. 133–161, https://doi.org/10.1007/978-1-4471-6584-2_7.

42. N. D. Skomrock, M. A. Schwemmer, J. E. Ting, H. R. Trivedi, G. Sharma, M. A. Bockbrader and D. A. Friedenberg, A characterization of brain–computer interface performance trade-offs using support vector machines and deep neural networks to decode movement intent, *Front. Neurosci.* **12** (2018) 763, doi: 10.3389/fnins.2018.00763.

43. Statistics and Machine Learning Toolbox, https://es. mathworks.com/help/stats/index.html?s_tid= CRUX_lftnav.

44. Lite, https://www.tensorflow.org/lite/microcontrollers.

45. E. Alpaydin, *Introduction to Machine Learning* (MIT Press, Massachusetts, 2020).

46. V. Vapnik, *The Nature of Statistical Learning Theory* (Springer Science & Business Media, New York, 1999).

47. E. M. Forney and C. W. Anderson, Classification of EEG during imagined mental tasks by forecasting with Elman recurrent neural networks, in *2011 Int. Joint Conf. Neural Networks*, 31 July – 5 August 2011, San Jose, CA, USA, pp. 2749–2755, doi: 10.1109/IJCNN.2011. 6033579.

48. S. Roy, A. Chowdhury, K. McCreadie and G. Prasad, Deep learning based inter-subject continuous decoding of motor imagery for practical brain–computer interfaces, *Front. Neurosci.* **14** (2020) 918.

49. J. Thomas, T. Maszczyk, N. Sinha, T. Kluge and J. Dauwels, Deep learning-based classification for brain–computer interfaces, in *2017 IEEE Int. Conf. Systems, Man, and Cybernetics (SMC)*, 5–8 October 2017, Banff, AB, Canada, pp. 234–239, doi: 10.1109/ SMC.2017.8122608.

50. M. H. Rafiei and H. Adeli, A new neural dynamic classification algorithm, *IEEE Trans. Neural Netw. Learn. Syst.* **28**(12) (2017) 3074–3083, doi: 10.1109/ TNNLS.2017.2682102.

51. K. M. Alam, N. Siddique and H. Adeli, A dynamic ensemble learning algorithm for neural networks, *Neural Comput. Appl.* **32**(10) (2020) 8675–8690.

52. J. Snoek, H. Larochelle and R. P. Adams, Practical Bayesian optimization of machine learning algorithms, *Adv. Neural Inf. Process. Syst.* **25** (2012).

53. J. Morrone and M. Lori, The interlinking of alpha waves and visuospatial cognition in motor-based domains, *Neurosci. Biobehav. Rev.* **149** (2023) 10515.

54. W. Klimesch, EEG alpha and theta oscillations reflect cognitive and memory performance: A review and analysis, *Brain Res. Rev.* **29**(2–3) (1999) 169–195.